Princeton Plasma Physics Laboratory

PPPL- 4724

PPPL- 4724

Kink Modes and Surface Currents Associated With Vertical Displacement Events

Janardhan Manickam, Allen Boozer and Stefan Gerhardt

February, 2012

Prepared for the U.S. Department of Energy under Contract DE-AC02-09CH11466.

Princeton Plasma Physics Laboratory
Report Disclaimers

Full Legal Disclaimer

This report was prepared as an account of work sponsored by an agency of the United States Government. Neither the United States Government nor any agency thereof, nor any of their employees, nor any of their contractors, subcontractors or their employees, makes any warranty, express or implied, or assumes any legal liability or responsibility for the accuracy, completeness, or any third party's use or the results of such use of any information, apparatus, product, or process disclosed, or represents that its use would not infringe privately owned rights. Reference herein to any specific commercial product, process, or service by trade name, trademark, manufacturer, or otherwise, does not necessarily constitute or imply its endorsement, recommendation, or favoring by the United States Government or any agency thereof or its contractors or subcontractors. The views and opinions of authors expressed herein do not necessarily state or reflect those of the United States Government or any agency thereof.

Trademark Disclaimer

Reference herein to any specific commercial product, process, or service by trade name, trademark, manufacturer, or otherwise, does not necessarily constitute or imply its endorsement, recommendation, or favoring by the United States Government or any agency thereof or its contractors or subcontractors.

PPPL Report Availability

Princeton Plasma Physics Laboratory:

http://www.pppl.gov/techreports.cfm

Office of Scientific and Technical Information (OSTI):

http://www.osti.gov/bridge

Related Links:

U.S. Department of Energy

Office of Scientific and Technical Information

Fusion Links

Kink modes and surface currents associated with Vertical Displacement Events

Janardhan Manickam, Allen Boozer*and Stefan Gerhardt

Princeton Plasma Physics Laboratory

Princeton Umiversity

Princeton, NJ

manickam@pppl.gov

PAC. 52.35Py, 52.30Fa, 52.55Tn, 52.65Kj

January 29, 2012

Abstract

The fast termination phase of a Vertical Displacement Event, VDE, in a tokamak, is modeled as a sequence of shrinking equilibria, where the core current profile remains constant so that the safety-factor at the axis, q_{axis}tedi, remains fixed and the q_{edge} systematically decreases. At some point the $n = 1$ kink mode is destabilized. When the growth-rate is small, the discharge remains in equilibrium due to self-induced surface currents, When the growth-rate is large the instability leads to the final disruption. In most cases this occurs when q_{edge} is slightly less than two and the kink mode is characterized by $m/n = 2/1$, where m and n are the poloidal and toroidal mode numbers. The surface current needed to maintain equilibrium is determined from the MHD

*Also at the Department of Applied Physics and Applied Mathematics, Columbia University, New York, NY 10027

perturbation and provides an estimate of the available curremt drive. An applicaton to NSTX provides favorable comparison with non-axisymmetric halo-current measurements. The model is applied to ITER and shows that the 2/1 mode is projected to be the most likely cause of the final disruption.

1 Introduction

Tokamak plasmas are inherently susceptible to an axisymmetric vertical instability, particularly when they are elongated. Consequently, normal plasma operation requires feedback control of the vertical position to counter the growth of small displacements. However circumstances such as improper or inadequate feedback control may lead to Vertical Displacement Events, VDEs, which often culminate in disruptions. The disruption occurs on a fast time scale and carries the potential of inducing large forces on the surrounding structures, within the vessel. Understanding the unstable mode-structure and related surface currents could help ameliorate the consequences of this dangerous event. This report addresses the ideal kink stability of the discharge, starting from the initial uncontrolled vertical displacement, upto the final current quench. The vertical motion is related to the axisymmetric, $n = 0$, instability, and the disruption generally has $n = 1$, here n is the toroidal mode number,

VDEs start with a vertical displacement, which may be upward or downward, but always pushing the plasma towards some material surface. Once contact is established, the plasma starts to shrink. This process continues until the onset of a fast growing instability leads to a current quench and termination of the discharge. The instability corresponds to an $n = 1$ kink mode, see reference [1].

The VDE evolves on a transport time-scale, significantly, slower than the fast, Alfvenic time-scale of the ideal kink instability. This implies that during most of the VDE, the shrinking plasma is in equilibrium and should be kink stable, until the time of the disruption. Shortly before the disruption, currents are observed in the halo current monitors. These have been determined to have an axisymmetric, $n = 0$, as well as an $n = 1$, non-axisymmetric component.

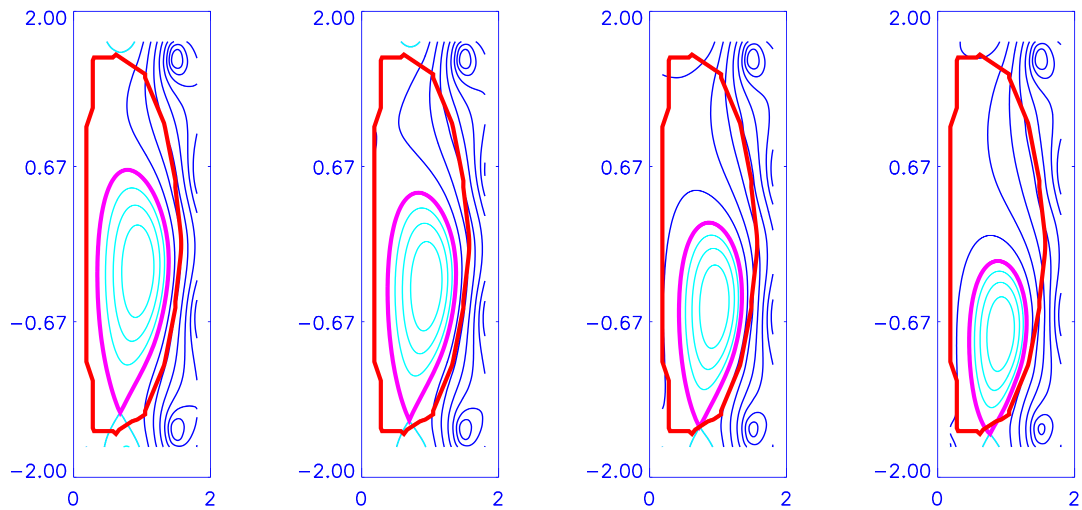

Figure 1: Equilibrium sequence of a VDE in an NSTX discharge, Shot No. 139540, at 3 *msec.* intervals starting at $t = 0.322$ seconds into the discharge. The discharge terminated at about $t = 0.338s$. The last usable equilibriun was at $t = 0.331s$. This was used to simulate the disruption phase. The last closed flux surface is highlighted in magenta

The latter may be related to the observed strong non-symmetric forces acting on the nearby conducting structures and vacuum vessel. This report addresses the ideal MHD stability of the plasma during the VDE, focusing on the $n = 1$ mode, its growth-rate and associated surface currents.

A theoretical model has emerged connecting the equilibrium of a kink-deformed plasma, with currents on the plasma surface,[2, 3, 4]. These currents flow parallel to the field, and counter to the core plasma current. The plasma deformation is driven by a kink instability, and estimates of these currents can be obtained by determining the δ-function surface current required to ensure $\mathbf{B} \cdot \mathbf{n} = \mathbf{0}$, on the plasma-vacuum interface.. This report extends previous theoretical analyses, which was confined to cylindrical, Shafranov, plasma models, to numerical modeling of realistic plasmas based on experimental observations. A detailed study is presented of an NSTX discharge, using the best estimates of plasma profiles from experimental observations and modeling. This is followed by an application to ITER, using an equilibrium based on transport simulation. Results in JET geometry are also presented. The main results describe the onset conditions for the disruption and estimates of the surface current.

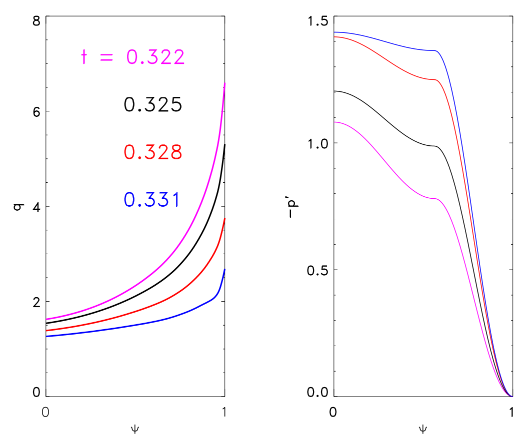

Figure 2: The plasma profiles for the safety-factor q and negative of the pressure gradient, $\frac{-dP}{d\psi}$, for the four cases, shown in Fig. 1. Note that as the plasma shrinks, q_{edge} reduces and approaches 2.0.

A comprehensive model requires the use of non-linear time-dependent MHD codes, coupled to a transport code treating the plasma, halo and material surfaces self-consistently. Research along these lines is still evolving and has provided insight on this complex problem, particularly relating the instability to the forces within the machine. [5].

This study is based on a simple linear ideal MHD model. However it provides meaningful information on stability boundaries, mode structures and growth-rates. In particular, since the growth-rate is a measure of the energy released by the instability, it provides a window on the forces involved.

The following sections describe: the plasma model, a method to determine the surface currents; application to NSTX; the results for ITER and JET geometries; and conclusions.

2 Plasma model

The evolution of the VDE is described by a sequence of plasma equilibria, with shrinking boundaries as the outer flux surfaces are lost, the safety-factor at the plasma boundary reduces continuously. These features are shown in Figure 1. The equilibria were reconstructed using LRDFIT, [6], for NSTX shot number 139540 at 3 *msec* intervals, starting at $t = 0.322$ *secs*. Figure 2 shows details of the safety factor and pressure gradient profiles for the equilibria in Fig. 1. Figure 3 shows the evolution of q_{edge} and the normalized beta, β_{N}, as well as the plasma current, I_p, and the measured 'halo' currents. These are seperated into the axisymmetric, $n = 0$ and non-axisymmetric $n = 1$ components.

We note that q_{edge} steadily decreases, dropping below 2 at $t = 0.3325s$. The halo currents are first observed at $t = 0.331s$., and the plasma current starts to collapse at about $t = 0.334s$ just as the halo current approaches its peak. Note that the entire event evolves over approximately 8 *msec*, a time scale which is much longer than the Alfvén time.

Ideally, for stability analysis, a sequence of plasma equilibria should be computed by fitting experimental data at time-slices close to the final disruption. This is not always possible as the experimental diagnostics may not be tuned to the shifting plasma location and key diagnostics may not be triggered in a timely manner. To overcome this we have developed

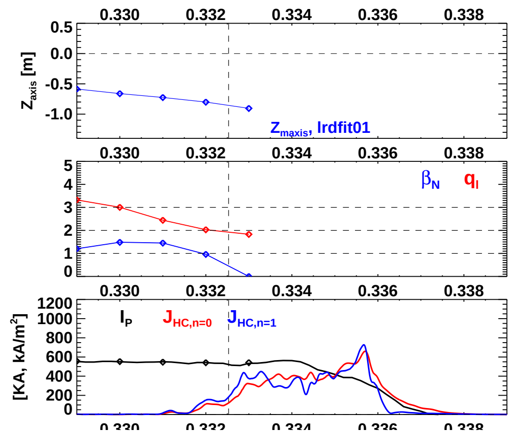

Figure 3: Evolution of Z_{axis}(top panel), q_{edge} and β_N,(middle panel) during the last 15 milli-seconds of a VDE in NSTX, Shot No. 141641. b. The plasma current, black, and halo current measurements for $n = 0$, red; and $n = 1$, blue are shown in the bottom panel. Note that q_{edge} is continuously decreasing and drops below 2 at approximately $t = 0.332s$., The halo current saturates at that time, and the disruption follows at $t = 0.335s$.

a model to mimic this sequence. We start from the closest valid equilibrium, representing a stable point, before the disuption. Starting from this equilibrium, a sequence of equilibria is generated as follows,

- Select an inner flux surface from the equilibrium, obtain the **x,z** values, to be used as the plasma

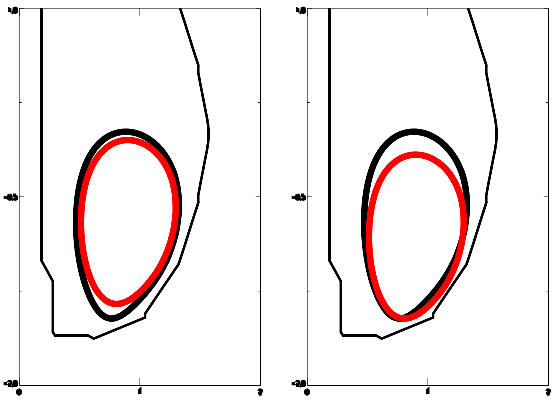

Figure 4: Method used to extend the equilibrium sequence to simulate the disruption phase. A selected inner flux surface is shifted to represent the new bounding surface for a new fixed-boundary equilibrium calculation. The figure on the left shows the 99% flux surface in black, at $t = 0.331$ and $q_{edge} \approx 2.5$, and an inner flux surface corresponding to $q_{edge} \approx 2.1$. The figure on the right shows the 2.1 surface displaced downwards to rest against the limiter(not shown). The curves overlap, on the right because the inner flux surface shape has reduced triangularity.

boundary of a new equilibrium, e.g.,

$$\Psi_b = b * (\Psi_{\rm lim} - \Psi_{\rm axis})$$

where $0.0 < b < 1.0$.

- Truncate and renormalize the equilibrium profiles $< \mathbf{J} \cdot \mathbf{B} > / < \mathrm{B}^2 >$ and $\mathrm{dp}/\mathrm{d}\Psi$, eg. using $\chi = \Psi/\Psi_{\rm b}$, we interpolate the plasma functions as follows

$$f(\chi)(0:1) = f(\Psi)(0:\Psi_{\rm b})$$

- Use a fixed boundary equilibrium code, JSOLVER, [7], to obtain a numerical equilibrium

$$f(\chi)(0:1) = f(\Psi)(0:\Psi_{\rm b})x)$$

- Use a fixed boundary equilibrium code, JSOLVER, [7], to obtain a numerical equilibrium

This procedure is illustrated in Figure 4. The figure on the left shows a selected flux surface of the initial stable equilibrium. The surface is displaced downwards until it brushes against the limiter and used as the bounding surface in a fixed boundary equilibtium calculation.

The stability is determined using the PEST[8] code. The mode of interest is the $n = 1$ kink mode.

Most of the studies set an ideal wall congruent with the vacuum vessel, free boundary calculations were also performed.

3 Surface current calculation

A current flowing on a flux surface, ψ_s , has the general representation

$$\vec{j}_s = \vec{\nabla} \times (\kappa(\theta, \varphi)\vec{\nabla}\psi\delta(\psi - \psi_s)) \tag{1}$$

where κ is called the current potential and has units of amperes. The power that must be used to drive that current potential is

$$\frac{d\delta W}{dt} = -\int \vec{j}_s \cdot \vec{E} d^3x, \tag{2}$$

which can be rewritten using Faraday's law as

$$\begin{aligned} \frac{d\delta W}{dt} &= \int \kappa \frac{\partial \vec{B}}{\partial t} \cdot \vec{\nabla}\psi\delta(\psi - \psi_s)\mathcal{J} d\psi d\theta d\varphi & (3) \\ &= \oint \kappa \frac{\partial \vec{B}}{\partial t} \cdot d\vec{a} & (4) \end{aligned}$$

The normal magnetic field can be expanded in orthonormal functions as

$$\vec{B} \cdot \hat{n} = w \sum_j \Phi_j(t) f_j(\theta, \varphi) \tag{5}$$

where $\oint wda = 1$ is a weight function and the expansion functions are defined so

$$\oint f_j f_k w da = \delta_{jk}. \tag{6}$$

The area element is $da = |\vec{\nabla}\psi|\mathcal{J} d\theta d\varphi$, where $\mathcal{J}$ is the coordinate Jacobian, and $d\vec{a} = \hat{n} da$.

The power equation, Eq. 3, can then be written as

$$\frac{d\delta W}{dt} = \sum_j \frac{d\Phi_j}{dt} \oint \kappa f_j w da. \tag{7}$$

If the current potential is expanded in terms of the same orthonormal functions, $\kappa = \sum_j I_j(t) f_j(\theta, \varphi)$, the energy equation becomes

$$\begin{aligned} \frac{d\delta W}{dt} &= \sum_j \frac{d\Phi_j}{dt} I_j & (8) \\ &= \sum_{jk} \frac{d\Phi_j}{dt} \rho_{jk} \Phi_k, & (9) \end{aligned}$$

where the linearity of the problem was used to write $I_j = \sum_k \rho_{jk} \Phi_k$.

The energy required to reach a certain point on a path defined by specified $\Phi_j(t)$ is $\delta W = \sum_{jk} \Phi_j \rho_{jk} \Phi_k / 2$. This result depends on the path take through the space of the $\Phi_j(t)$ unless the matrix ρ_{jk} is symmetric as a differentiation, $d\delta W/dt$, of this expression for δW demonstrates. In ideal MHD the energy is path independent, so ρ_{jk} is symmetric, which means the left and right eigenvectors of ρ_{jk}

are identical. In other words, for a specific eigenvector of δW the same eignenfunction $f(\theta,\varphi)$ gives the flux and the current potential, and Equation (3) implies the energy associated with the eigenfunction is $\delta W = I\Phi/2$.

The energy for a specific ideal MHD mode has the form $\delta W = I\Phi/2$, so the current I is trivially calculated once Φ is know. Since $\vec{B}\cdot\hat{n} = w\Phi f$ and $\oint f^2 w da = 1$,

$$\Phi^2 = \oint \frac{(\vec{B}\cdot\hat{n})^2}{w} da. \qquad (10)$$

The normal component of the perturbed field, $\vec{Q} = \nabla\times\xi\times\vec{B}$, is given by,

$$\frac{\vec{Q}\cdot\nabla\psi}{|\nabla\psi|} = \frac{1}{R\mathcal{J}\nabla\psi|}\left(\frac{\partial\xi}{\partial\theta} + \frac{\partial\xi}{\partial\Phi}\right) \qquad (11)$$

Here, R, is the major radius, and $\mathcal{J}$, is the Jacobian. These are obtained from the post-processor of the PEST code [10].

Normalization in the cylindrical limit.

This approach, use of a linear model, requires additional information about the normalization. This is resolved by comparing with the cylindrical analytic

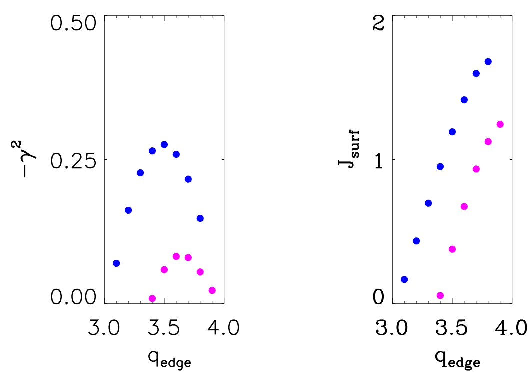

Figure 5: Growth-rate of the free boundary $n = 1$, kink mode for the 'cylindrical' model equilibria defined in Ref. [9], left panel. The blue dots correspond to $j_1 = 0.5$ and the magenta dots are for $j_1 = 0.25$b The corresponding values of j_{surf}, Eq. 20 of Ref [9] , right panel

model, described in Ref. [9].

Specifically, we approximate the straight system, with a circular cross-section tokamak with an aspect-ratio equal to twenty. The QSOLVER code[7], where the safety-factor and pressure profile, and plasma geometry are prescribed, was used to obtain numerical equilibria. A negligible, finite pressure was used, $\beta_{\rm N} \sim 0.1$. The safety-factor profile is prescribed as

$$\mu(r) = \frac{4\mu_a}{1+j_1}\left[\frac{1}{2} - (1-j_1)\frac{r^2}{4a^2}\right] \qquad (12)$$

with $\mu = 1/q$, μ_a defines the edge safety-factor and j_1 prescribes the shear. In the numerical simulation, we use a large, but finite aspect-ratio, set equal to twenty.

Stability analysis and surface current evaluation were done using the procedure, described above. The surface current, J_s, computed here is the same as $\hat{i}^{surf}$, Eqn. 20 of Ref. [9]. Note, that this is a dimensionless form and relates to the the ratio of the surface current to the plasma current and that of the displacement, ξ, relative to the plasma radius, a

$$\mu_0 \frac{I_s}{I_p} = \hat{i}^{surf} \frac{\xi}{a} \tag{13}$$

.

Ihe results shown in Fig. 5, compare favorably with the results shown in Figure 2 of Ref.[9]. Minor differences are attributable to the use of $f(\Psi)$ rather than $f(r)$, and the use of finite aspect ratio to represent the cylindrical limit.

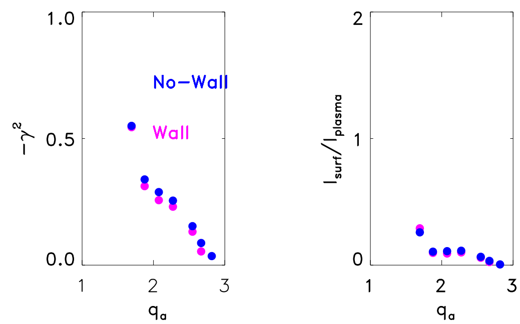

Figure 6: a. Growth-rate of the free boundary kink mode for the simulated equilibria of NSTX discharge 139540. Note, that the I_{surf} required to stabilize the mode, is modest until $q_{\rm edge}$ drops below 2

4 Results

NSTX results

Shot 139540. An NSTX discharge, 139540, which ended in a disruption at $t \sim 0.34s.$, was analyzed. Figure 3 shows some of the salient observations. The figure shows the measured plasma current, I_p, which remains roughly constant, until $t = 0.334s.$, and then drops to zero in 2 ms. This drop is heralded by a rise in the measured halo currents. The halo currents are identified as a combination of an axisymmetric, $n = 0$, and non-axisymmetric, $n = 1$ components. These currents reach values comparable to the plasma current:

$$0.2 \leq \frac{I_{surf}}{I_{plasma}} \leq 0.4 \tag{14}$$

. The normalized pressure, $\beta_{\rm N}$ and estimates of $q_{\rm edge}$

are also shown. Note that $q_{\rm edge}$ decreases continuously, crossing $q = 3$ at about

330 ms., and $q = 2$ at 332 ms., approximately coincidental with a significant rise in the halo current.

We model the disruption using the equilibrium corresponding to 331 ms. as the starting point. The modeling followed the procedure described in the section on plasma modeling. The results are shown n Fig. 6. A fast growing mode is observed when $q_{\rm edge}$ drops below 3, however the surface current required for equilibrium is quite modest until $q_{\rm edge}$ drops below 2. It should be noted that while $q_{\rm edge}$ is reasonably well determined, the details of the profile in the core are not as precise. The figure also shows growth-rates and current fractions with no-wall boundary coditions and with the wall congruent to the vacuum vessel. Since the plasma is shrunken and shifted, see right panel of fig. 4, the wall effect is negligible, for this case.

Shot 141641

This discharge had a slow VDE, lasting about 15 msecs. As the plasma drifts downwards, there is a significant rise in the halo currents, Fig. 7, which

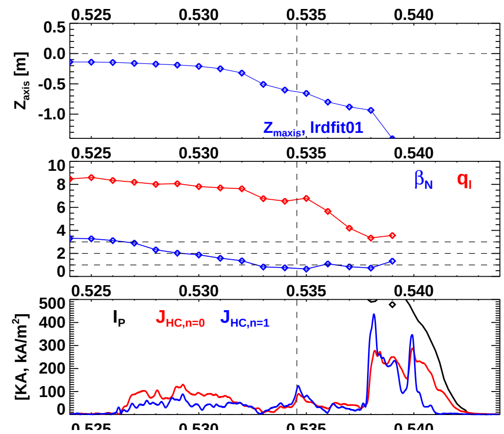

Figure 7: a. Evolution of Z_{axis}, $q_{\rm edge}$ and β_N, during the last 15 milli-seconds of a VDE in NSTX, Shot No. 141641. b. The plasma current, black, and halo current measurements for $n = 0$, red; and $n = 1$, blue. Note that $q_{\rm edge}$ is continuously decreasing and drops to approximately 3.5 at $t = 0.538s.$, The halo current is first observed at about $t = 0.527s.$, when q_{edge} 8.

lasts for well over 10 milliseconds. It is also unusual, as q_{edge} is above 6 at the start of the VDE, and the final disruption occurs when $q_{edge} \approx 3$. Using the same procedure, described earlier, theoretical modeling shows that the kink mode is destabilized at high-$q_{\rm edge}$ and the surface currents mimic the behavior of the measured halo currents, Figure 8.

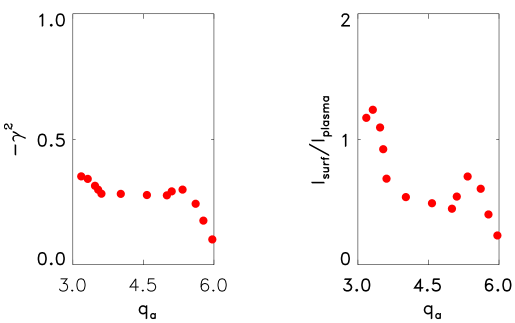

Figure 8: a. Growth-rate of the free boundary kink mode for the simulated equilibria of NSTX discharge 141641. Note, that this shot appears to survive for several milli-seconds after the onset of the kink, suggesting that the observed halo currents may be providing stability until q_{edge} approaches 3.

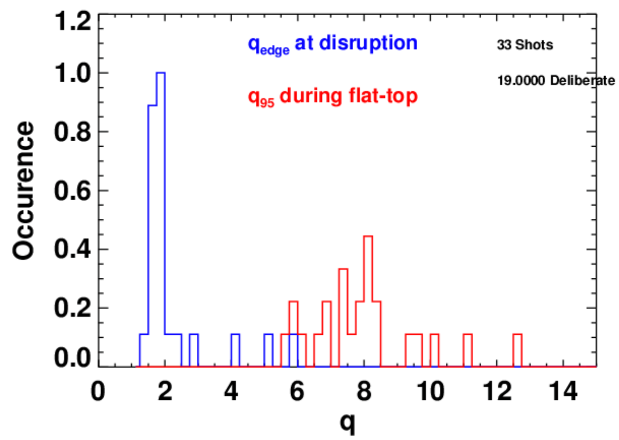

Figure 9: a. Frequency of fast disruptions in deliberately induced VDEs. The edge safety-factor at the onset of the VDE, flat-top, and at the final disruption are showm in *red* and *blue*, respectively. Note that $q_{\rm edge}$=2 is the most likely value at disruption.

We have compiled data from 33 discharges, which ended in disruptions. The modeling of $q_{\rm edge}$, just before disruption, indicates that the majority of these discharges disrupted as $q_{\rm edge}$ dropped below 2, see Fig.9.

The analysis of NSTX VDEs also indicates that when the kink mode's growth-rate is small, surface currents can provide stability, and disruptions occur only when $\gamma \rm T_A \sim 0.5$. Here $\rm T_A$ refers to the Alfvénic time, characteristic of ideal MHD instabilities.

ITER geometry

We applied the same techniques to predict the likely behavior of an ITER discharge. We used a simple low-β L-mode equilibrium, and generated a sequence of shrinking equilibria. The results are shown in Figure 10. Here too, we find that the equilibrium sequence is stable until $q_{\rm edge}$ drops below three, when a marginally unstable mode is observed at $q_{\rm edge}$ ~2.5. However, as q drops below two, the growth-rate increases dramatically approaching unity, on the Alfven time scale. The surface current needed to maintain equilibrium is also shown in Fig. 10.

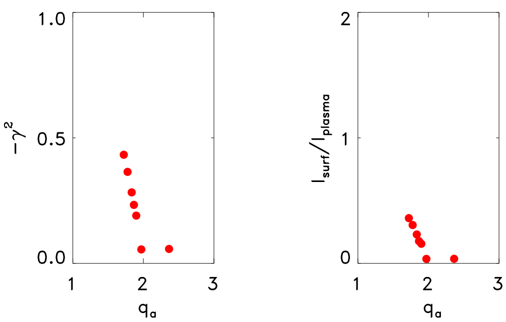

Figure 10: **a** Growth-rate of the free boundary $n = 1$, kink mode for ITER model equilibria. **b** The surface current required to maintain equilibrium.

JET geometry

Simulation of the linear stability of the $n = 1$ kink mode in JET geometry, shows similar results to the ITER case, *i.e.*, a rapid growth of the instability for q less than 2. However the mode is unstable for q larger than two. The surface current required for stability is approximately half the equilibrium plasma current, when $q_{\rm edge}$ drops below 2, Figure 11.

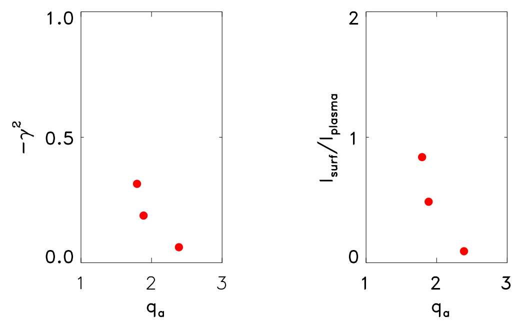

Figure 11: **a.** Growth-rate of the free boundary $n = 1$, kink mode for model equilibria, representing a VDE in JET geometry. **b** The surface current correponding to the $n = 1$ kink

5 Discussion

This report describes a practical approach to identifying the kink mode responsible for disruptions terminating some VDEs. Specifically it indicates that the $m/n = 2/1$ kink mode, destabilized when $q_{\rm edge} < 2$ is the most likely signature of the onset of a disruption.

A method for determining the surface currents needed to maintain equilibrium was presented. Applications were made to model VDEs in NSTX. There is good corelation of the $q_{\rm edge}$ and stability between experiment and theory. In addition, the calculated surface currents were observed to reach the same magnitude as measured halo currents, suggesting that the two are related.

Although this study predicts Alfvénic growth-times, the expectation is that a halo current will arise to maintain force balance and the actual evolution takes place on the dissipative time scale of that current. Nevertheless the mode's growth-rate is a measure of the strength of the instability, and the prescribed stability condition for the disruption is that the growth-rate is approximately half the Alfven time. This describes the onset of disruption, however the actual process is very likely. more complex and requires additional physics.

This study focused on VDE related disruptions. However the underlying theory should apply to all instabilities related to surface kinks, such as, high-beta kinks, RWMs and low-n ELMs. Evidence of such surface currents associated with ELMs was presented in Ref. [12], where the term SOLC, Scrape Off Layer Currents, was introduced. The theory presented here suggests that the SOLC may be the kink-driven surface currents. Another significant feature of this theory is that destabilization of the kink mode does not necessarily lead to an immediate termination of the discharge. Surface currents can provide a delayed response, if so, it raises the possibility of detecting SOL currents as a disruption precursor. We have examined the data base and observed that nearly all NSTX disruptions have some precursor, such as degradation of the confinement, increased flux consumption and large-scale MHD activity. Additionally, we often see a large spike in the halo current monitors a few *msecs* before the disruption, before there is any large vertical motion of the plasma. Further studies are required to determine if the SOL currents can be used as reliable disruption precursors.

Acknowledgements. This study benefited from Dr. L. Zakharov's insights on understanding and modeling disruptions in tokamaks.This manuscript has been authored by Princeton University and collaborators under Contract Number(s) DEAC0209CH11466 with the U.S. Department of Energy. The publisher, by accepting the article for publication, acknowledges that the United States Government retains a nonexclusive, paidup, irrevo-

cable, worldwide license to publish or reproduce the published form of this manuscript, allow others to do so, for United States Government purposes.

References

[1] "ITER Physics Basis", Nuclear Fusion **39**, 2137 (1999).

[2] L. Zakharov Physics of Plasmas, **15**, 062507 (2008).

[3] R. Fitzpatrick, Physics of Plasmas, **16**, 012506 (2009).

[4] A. J. Webster, Physics of Plasmas, **17**, 110708 (2010).

[5] H. R. Strauss, R. Paccanella, and J. Breslau, **17**, 082105, (2010).

[6] J. Menard Physics of Plasmas, **14**, p. 18 (2007).

[7] J. Delucia, S. C. Jardin and A. M. M. Todd, J. Comp. Phys. **37**, 183-204(1980).

[8] R. C. Grimm, J. M. Greene, J. L. Johnson, Methods in Comp. Phys. **16**, 253 (1976).

[9] L. Zakharov Physics of Plasmas, **18**, 062503 (2011).

[10] S. Preische, J. Manickam and J. L. Johnson, Comp. Phys. Comm.**76**, 318-325, (1993).

[11] S. P. Gerhardt, E. D. Fredrickson, L. Guttadora, H. Kugel, J. Menard and H. Takahashi, Rev. Sci. Instr., Phys. Rev. Letters, **82** , 133508 (2011).

[12] H. Takahashi, E. D. Fredrickson and M. J. Schaeffer Phys. Rev. Letters, **100** , 205001 (2008).

The Princeton Plasma Physics Laboratory is operated
by Princeton University under contract
with the U.S. Department of Energy.

Information Services
Princeton Plasma Physics Laboratory
P.O. Box 451
Princeton, NJ 08543

Phone: 609-243-2245
Fax: 609-243-2751
e-mail: pppl_info@pppl.gov
Internet Address: http://www.pppl.gov